Dissolution of Latex Films After γ-ray Treatment

K. AYDIN, N. ADIYAMAN, Ş. UĞUR, Ö. PEKCAN

Department of Physics, Istanbul Technical University, Maslak, 80626 Istanbul, Turkey

Received 30 June 2000; accepted 2 March 2001

ABSTRACT: Latex films were prepared by annealing pyrene (Py)-labeled poly(methyl methacrylate) particles at glass-transition temperature (100°C). These films were then irradiated by γ-rays from ^{60}Co in a gamma cell at room temperature at the same dose rate (rad/h) for 30 min. Before dissolution films were annealed at elevated temperatures for a 30-min time interval to complete the film formation process. Steady-state fluorescence (SSF) technique were used to monitor the dissolution of these irradiated latex films. The dissolution of films in chloroform–heptane (80–20%) mixture was monitored in real time by the Py fluorescence intensity change. Relaxation constants k_0 and desorption coefficients D_d of polymer chains were measured. It was observed that both D_d and k_0 values first increased and then decreased by increasing the annealing temperature. © 2002 John Wiley & Sons, Inc. J Appl Polym Sci 83: 129–137, 2002

Key words: latex films; γ-ray treatment; latex dispersion; desorption; steady-state fluorescence; interdiffusion

INTRODUCTION

In general aqueous or nonaqueous dispersion of colloidal particles with glass-transition temperature (T_g) above the drying temperature is named high-T_g latex dispersion; however, aqueous dispersion of colloid particles with T_g below the drying temperature is called low-T_g latex dispersion. The term "latex film" normally refers to a film formed from low-T_g particles, in which the forces accompanying the evaporation of water are sufficient to compress and deform the particles into a transparent, void-free film.[1,2] However, high-T_g latex particles remain essentially discrete and undeformed during the drying process. Latex films can also be obtained by compression molding of a dried latex powder composed of polymers such as polystyrene (PS) or poly(methyl methacrylate) (PMMA) that has T_g above room temperature. Film formation from these dispersions can occur in several stages. In both cases stage I corresponds to the wet initial state. Evaporation of solvent leads to stage II, in which the particles form a closed packed array, such that if the particles are soft they are deformed to polyhedrons. Hard latex, however, remains undeformed at this stage. Annealing of low-T_g particles causes diffusion across particle–particle boundaries, which leads to void closure, and then after the voids disappear diffusion across particle–particle boundaries starts.[3,4] In other words void closure is the rate-limiting step for film formation from hard latex particles.[5]

Polymer latex is an important industrial product and its film-formation process has therefore been the subject of much theoretical and experimental attention. Transmission electron microscopy (TEM) has been the most common technique used to investigate the structure of dried films.[6,7] A pattern of hexagons, consistent with face-centered cubic packing, is usually observed in highly ordered films. When these films are annealed, the complete disappearance of structure is sometimes observed, which is consistent with extensive polymer interdiffusion. Freeze-fracture TEM

Correspondence to: Ö. Pekcan.

Journal of Applied Polymer Science, Vol. 83, 129–137 (2002)

(FFTEM) has been used to study the structure of dried latex films.[8,9] Small-angle neutron scattering (SANS) has been used to study latex film formation at the molecular level. Extensive studies using SANS have been performed by Sperling and coworkers[10] on compression-molded PS film. The direct nonradiative energy transfer (DET) method has been employed to investigate the film-formation processes from dye-labeled high-T_g[11] and low-T_g[12,13] polymeric particles. The steady-state fluorescence (SSF) technique combined with DET was used to examine both healing and interdiffusion processes in dye-labeled high-T_g latex systems.[14–18] Recently, a UV–visible technique was used to study film formation from both high-T_g and low-T_g latex particles.[19–21]

Radiation can be used to change the physical properties of polymeric systems, given that crosslinking and chain scission cause alterations in the average molar mass and other important physical properties depend on the molar mass. It is well known that crosslinking commonly exerts desirable effects on mechanical properties up to a certain absorbed radiation dose. In other words, up to a certain degree of crosslinking, chain scission leads to severe property deteriorations immediately after the irradiation has started. Irradiation of polymers to high absorbed doses is always undesirable because it causes embrittlement and color changes.[22] Several sources can be used to produce electromagnetic radiations in various wavelengths. Commercially available lamps such as deuterium, xenon, or mercury lamps serve as sources for low-energy electromagnetic radiation in the UV–visible region. Solid-state and gas lasers producing monochromatic and coherent light covering the range of UV to IR are used as radiation sources. X-rays can be produced by commercially available tubes for powerful X-ray sources, and electron synchrotrons are used to generate high-energy electromagnetic radiations. α- and β-rays as well as heavy-ion energies ranging up to several hundred eV can be produced by particle accelerators, and neutron beams are available in nuclear reactions (rays can be obtained from simple sources such as ^{60}Co).

The penetration of solvent molecules into glassy polymers often does not proceed according to the Fickian diffusion model.[23–27] Penetration that is not described by the Fickian model is called anomalous diffusion, in which the rate of transport is entirely controlled by polymer relaxation. This transport mechanism is termed Case II, in contrast to Fickian diffusion, which is called Case I. It is well known that polymeric films dissolve mainly in four sequential steps: (1) solvent penetration, (2) polymer relaxation, (3) desorption of polymer chains into the solvent reservoir, and (4) chain diffusion in solvent. In the Case II diffusion model, the second step is the rate-limiting step, which predicts a linear dependency of the change in film thickness on time. The first and third steps, however, follow a Case I diffusion model, in which the first step is the absorption of solvent molecules by the glassy film and the third is the desorption of polymer chains from the gel layer. The fourth and final step of polymer dissolution involves the diffusion of polymer molecules throughout the liquid phase.

Polymer films obtained from latex particles are usually used for their resistance to permeation by organic solvents, water, oxygen, and other corrosive agents. Consequently, dissolution of polymers in organic solvents has attracted attention for the photoresist dissolution process in integration circuits.[28–30] In controlled release applications of polymers a solute is dispersed or molecularly dissolved in a polymer phase.[31] The release process can be controlled either by solvent diffusion or by polymer dissolution. Poly(methyl methacrylate) (PMMA) film dissolution was first studied using laser interferometry by varying molecular weight and solvent quality.[32] Winnik and coworkers[30] modified the interferometric technique and studied the dissolution of fluorescence-labeled PMMA films by monitoring the intensity of fluorescence from the film together with the interferometric signal. The solvent penetration rate into the film and the film dissolution were measured simultaneously. Fluorescence quenching and depolarization methods have been used for penetration and dissolution studies in solid polymers.[33–35] The real-time, nondestructive method for monitoring small molecule diffusion in polymer films has been developed.[36–39] This method is based on the detection of excited fluorescence dyes desorbing from a polymer film into a solution in which the film has been placed. Recently, we reported an SSF study on the dissolution of both annealed latex film[40] and PMMA discs using real-time monitoring of fluorescence probes.[41,26]

The polymer dissolution process can be affected by various parameters, including solvent quality, polymer molecular weight, solvent thermodynamic compatibility, agitation, and temperature. In this work, the effect of γ-irradiation on the latex film dissolution process was studied using

the SSF method by real-time monitoring of the pyrene (Py) intensity change. A chloroform–heptane (80–20%) mixture was used as the dissolution agent. *In situ* SSF experiments were performed to observe the dissolution processes. Dissolution experiments were designed so that Py-labeled polymer chains desorbing from films were detected in real-time monitoring of SSF intensity. Desorption coefficients D_d and relaxation constants k_0 were measured using curves of Py intensity versus time by using Case I and Case II diffusion models. D_d values were found to range between 9 to 21 $\times$ 10^{-10} cm^2 s^{-1} and k_0 values were measured from 3 to 6 $\times$ 10^{-1} mg cm^{-2} min^{-1}.

CASE I AND CASE II DIFFUSIONS

Various mechanisms and various mathematical models have been considered for polymer dissolution. Quano[42] proposed a model that includes polymer diffusion in a liquid layer adjacent to the polymer and moving of the liquid–polymer boundary. The key parameter for this model was the polymer dissociation rate, defined as the rate at which polymer chains desorb from the gel interface. Peppas[43] extended this model for films to the situations of the polymer dissolution rate where gel thickness was found to be proportional to $(\text{time})^{1/2}$. A relaxation-controlled model was proposed by Brochard and de Gennes[44] in which, after a swelling gel layer was formed, desorption of polymer from the swollen bulk was governed by the relaxation rate of the polymer stress. This rate was found to be of the same order of magnitude as the reptation time. The dependencies of the radius of gyration and the reptation time on polymer molecular weight and concentration were studied, using a scaling law[45] based on the reptation model.

In this study we employed a simpler model, developed by Enscore et al.,[23] to interpret the results of polymer swelling and dissolution experiments. This model includes Case I and Case II diffusion kinetics. The Case I model is the solution of a unidirectional diffusion equation for a set of boundary conditions, as cited by Crank.[46] For a constant diffusion coefficient D and fixed boundary conditions, the sorption and desorption transport in and out of a thin slab is given by the following relation:

$$\frac{M_t}{M_\infty} = 1 - \frac{8}{\pi^2} \sum_{n=0}^{\infty} \frac{1}{(2n+1)^2} \exp\left(\frac{-(2n+1)^2 D \pi^2 t}{d^2}\right) \tag{1}$$

Here, M_t represents the amount of materials absorbed or desorbed at time t, $M_{[\text{yen}]}$ is the equilibrium amount of material, and d is the thickness of the slab.

The Case II transport mechanism is characterized by the following steps. As the solvent molecules enter into the polymer film, a sharp advancing boundary forms and separates the glassy part of the film from the swollen gel. This boundary moves into the film at a constant velocity. The swollen gel behind the advancing front is always at a uniform state of swelling and its thickness stays constant during dissolution. Solvent penetration, formation of the gel layer, and propagation of the gel layer and desorption of polymer chains are presented in Figure 1(a)–(c), respectively. Now, consider a cross section of a film with thickness d, undergoing Case II diffusion, in which L is the position of the advancing sorption front, C_0 is the equilibrium penetrant concentration, and k_0 (mg cm^2 min^{-1}) is defined as the Case II relaxation constant. The kinetic expression for the sorption in the film slab of an area A is given by

$$\frac{dM_t}{dt} = k_0 A \tag{2}$$

The amount of penetrant M_t absorbed in time t will be

$$M_t = C_0 A(d - L) \tag{3}$$

After eq. (3) is substituted into eq. (2) the following relationship is obtained:

$$\frac{dL}{dt} = -\frac{k_0}{C_0} \tag{4}$$

It can be seen that the relaxation front, positioned at L, moves toward the origin with a constant velocity, k_0/C_0. The algebraic relation for L, as a function of time t, is described by eq. (5):

$$L = d - \frac{k_0}{C_0} t \tag{5}$$

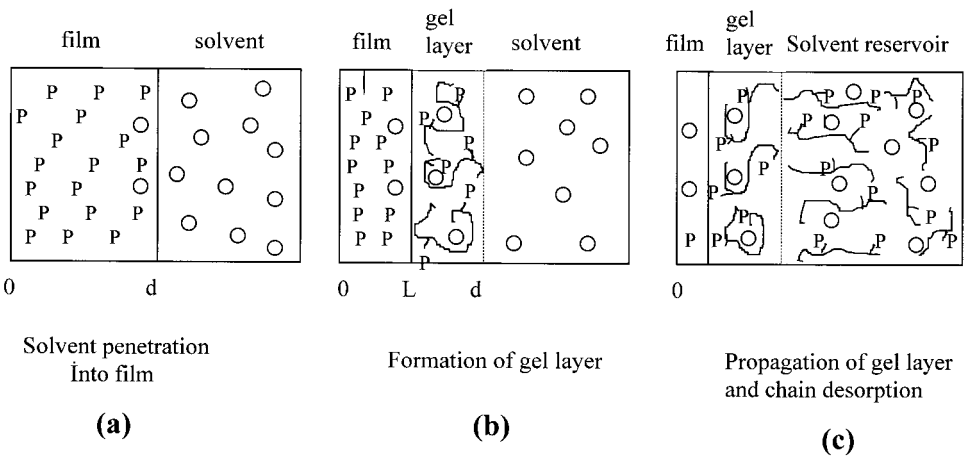

Figure 1 Dissolution of film: (a) solvent penetration, (b) formation of gel layer, (c) propagation of gel layer and chain desorption.

Given that $M_t = k_0 A_t$ and $M_{[yen]} = C_0 A_d$, the following relationship is obtained:

$$\frac{M_t}{M_\infty} = \frac{k_0}{C_0 d} t \tag{6}$$

EXPERIMENTAL

Pyrene (Py)-labeled PMMA–PIB latex particles were prepared separately in a two-step process in which MMA in the first step was polymerized to low conversion in cyclohexane in the presence of PIB containing 2% isoprene units to promote grafting. The graft copolymer so produced served as a dispersant in the second stage of polymerization, in which MMA was polymerized in a cyclohexane solution of polymer, details of which were published elsewhere.[47] A stable spherical latex dispersion of polymer particles was produced, ranging in radius from 1 to 3 μm. A combination of ^{1}H-NMR and UV analysis indicated that these particles contain 4 mol % PIB and 0.037 mmol Py groups per gram of polymer. (These particles were prepared in M. A. Winnik's Lab in Toronto.) The molecular weight of the graft copolymer was found to be 2.5×10^5 g mol^{-1}.

Latex film preparation was carried out in the following manner. The Py-labeled particles were dispersed in heptane in a test tube. After complete mixing, a large drop of the dispersion was cast onto a glass plate the size of which was 2.5 $\times$ 0.8 cm^2. The heptane was allowed to evaporate. Eight films were prepared in the similar way. These films were then irradiated in a Gammacell with ^{60}Co γ-irradiator at room temperature at a dose rate of 1.32×10^3 rad. Irritated films were than annealed at elevated temperatures from 140 to 260°C for a 30-min time interval before dissolution.

In situ dissolution experiments were performed using a Perkin–Elmer LS-50 spectrofluorimeter (Perkin Elmer Cetus Instruments, Norwalk, CT). All measurements were made at a 90° position and the slit widths were kept at 8 mm. Dissolution experiments were performed in a 1 $\times$ 1-cm quartz cell that was placed in the spectrofluorimeter. The fluorescence emission was monitored so that film samples were not illuminated by the excitation light. Film samples were placed at one side of a quartz cell filled with a chloroform–heptane mixture (80–20%) and the cell was then illuminated with a 345-nm excita-

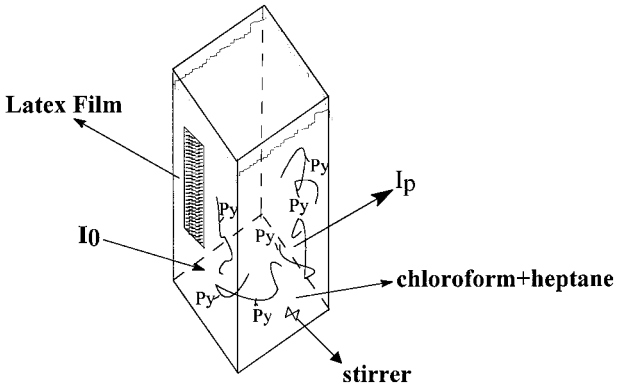

Figure 2 Dissolution cell in LS-50 Perkin–Elmer spectrofluorimeter. I_0 and I_P are the excitation and emission intensities at 345 and 395 nm, respectively.

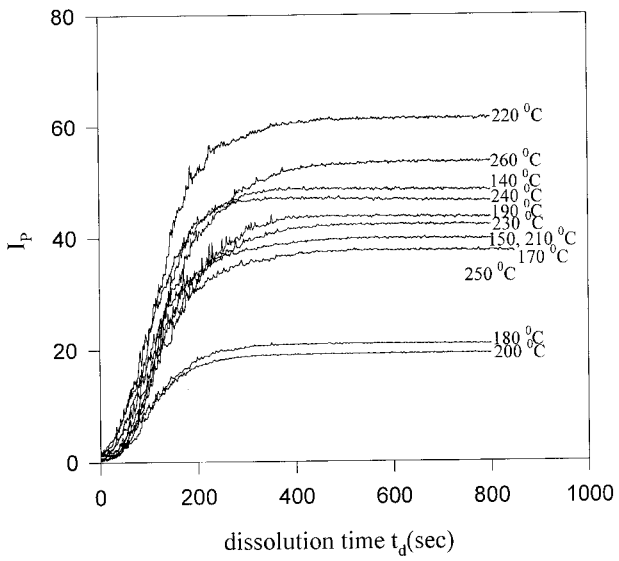

Figure 3 Pyrene intensities I_P versus dissolution time for the films irradiated at a dose rate of 1.32×10^3 rad and annealed at elevated temperatures. Numbers on each curve represent the annealing temperatures.

tion light. The position of the irradiated films and the excitation and emission light are presented in Figure 2. The pyrene fluorescence intensity I_P was monitored during the dissolution process at 395 nm using the "time drive" mode of the spectrofluorimeter. Emission of Py was recorded continuously at 395 nm as a function of time. Here the 1 × 1-cm quartz cell was equipped with a magnetic stirrer at the bottom. The Py fluorescence emission was monitored at a 90° angle, as shown in Figure 2.

RESULTS AND DISCUSSION

Plots of Py intensity I_P versus dissolution time for films annealed at different temperatures at low stirring speed are shown in Figure 3. Experimental conditions are listed in Table I. It is seen that all curves increase at early times by reaching plateau at later times. The curves in Figure 3 seem to follow a Case I (Fickian) diffusion model except at early times. In processing the dissolution data, it is assumed that I_P is proportional to the number of Py-labeled chains desorbing from the gel layer of PMMA film. Because the thickness of the gel layer stays constant during the dissolution of polymer film, eq. (1) turns out to be the solution of the moving slab problem. Here, because the solvent reservoir is considered to be infinitely large (see Fig. 2), the above assumption can be used to employ eq. (1). The logarithmic form of eq. (1) is written for $n = 0$, with $A_d = D_d\pi^2/(d - L)^2$ and $B_d = \ln(8/\pi^2)$ as follows:

$$\ln\left(1 - \frac{I_p}{I_{p\infty}}\right) = B_d - A_d t \tag{7}$$

Table I Experimentally Observed Parameters[a]

T (°C)	d (μm)	$t_{d\infty}$ (s)	t_L (s)	v (cm s^{-1}) ($\times 10^{-6}$)	L (μm)	$(d - L)$ (μm)	D_d (cm^2 s^{-1}) ($\times 10^{-10}$)	k_0 (mg cm^{-2} min^{-1}) ($\times 10^{-2}$)
140	10	400	100	2.5	2.5	7.5	8.4	8.7
150	11	500	100	2.6	2.2	8.8	8.1	9.3
160	10	400	100	2.5	2.5	7.5	8.8	8.0
170	11	500	100	2.2	2.2	8.8	7.7	9.2
180	13	400	100	3.2	3.2	9.7	12.0	15.5
190	11	500	150	2.2	3.3	7.7	9.0	12.6
200	13	400	100	3.2	3.2	9.7	11.7	13.3
210	11	450	100	2.4	2.4	8.5	11.6	13.3
220	13	475	125	2.7	3.4	9.6	10.8	11.2
230	12	500	100	2.4	2.4	9.6	10.9	8.2
240	10	400	100	2.5	2.5	7.5	10.1	7.6
250	10	350	75	2.8	2.1	7.8	9.9	14.7
260	10	650	120	1.5	1.8	8.2	6.3	5.7

[a] T, annealing temperature; d, film thickness (as seen in Fig. 1); $t_{d\infty}$, dissolution time of the film obtained from Figure 4; t_L, gel formation time obtained from Figure 5(a)–(c); $v = d/t_{d\infty}$, dissolution speed; $L = vt_L$, initial position of the gel front (as seen in Fig. 1); $(d - L)$, initial thickness of the gel layer (as seen in Fig. 1); D_d, desorption coefficient obtained using eq. (1); k_0, relaxation constant obtained using eq. (8).

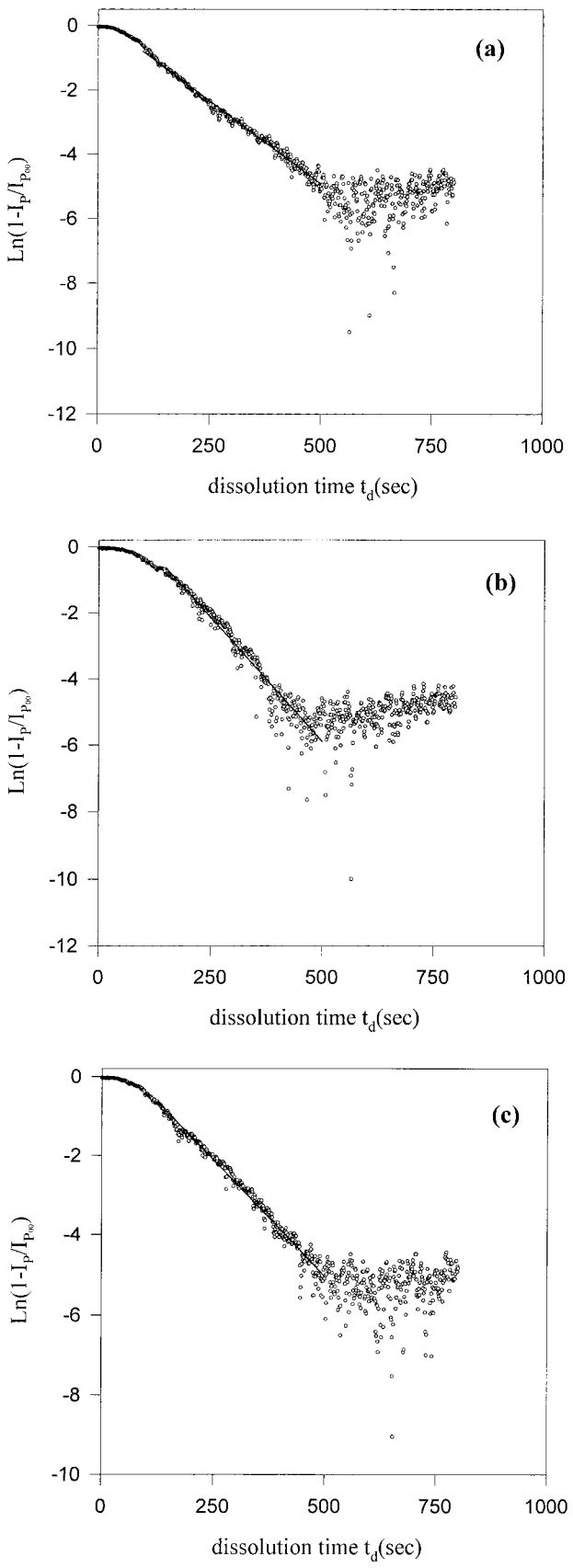

Here, $I_{p\infty}$ presents the number of Py-labeled chains at equilibrium condition, D_d is the desorption coefficient, and $(d - L)$ is the initial thickness of the gel layer, which remains constant during dissolution. $(d - L)$ values are estimated by knowing the film thickness (d) and the final dissolution time $(t_{d\infty})$. The dissolution speed v can then be calculated, which can then be used to estimate the initial position of the gel front L, if one knows the gel formation time t_L. The estimated $(d - L)$ values together with $t_{d\infty}$, v, t_L, and L are listed in Table I. Dissolution curves for temperatures of 150, 190, and 230°C are presented in Figure 4(a)–(c), respectively, which are digitized for numerical treatment according to eq. (7). When these linear curves in Figure 4(a)–(c) are compared to computations using eq. (7), desorption coefficients D_d of Py-labeled polymer molecules are obtained. These are listed in Table I and are plotted against annealing temperature [see Fig. 6(a) below]. Here higher values of dissolution coefficient D_d at the intermediate temperatures most probably belong to the PMMA chains in lower molecular weight, which are produced as a result of chain scission during irradiation. At higher annealing temperatures, however, chains combine and/or branch to form large molecules. These films dissolve much more slowly and, as a result, D_d values are found to be smaller. At low annealing temperatures, the small D_d values were something of a surprise and somewhat difficult to explain at this stage of the experiments.

Curves in Figure 3 at very short times are plotted in Figure 5(a)–(c) according to eq. (6). Here it is assumed that the amount of chloroform molecules entering into the latex film at early times is proportional to the number of PMMA chains desorbing from the swollen gel. Now eq. (6) becomes

$$\frac{I_P}{I_{P\infty}} = \frac{k_0}{C_0 L}\, t \tag{8}$$

Fitting eq. (8) to the data presented in Figure 5(a)–(c) produced the k_0 parameters, which are listed in Table I and plotted in Figure 6(b), where

Figure 4 The logarithmic plot of the curves in Figure 3 and their fits according to eq. (7) for the films annealed at (a) 150°C, (b) 190°C, and (c) 230°C. From the slopes of these curves dissolution coefficients D_d can be obtained.

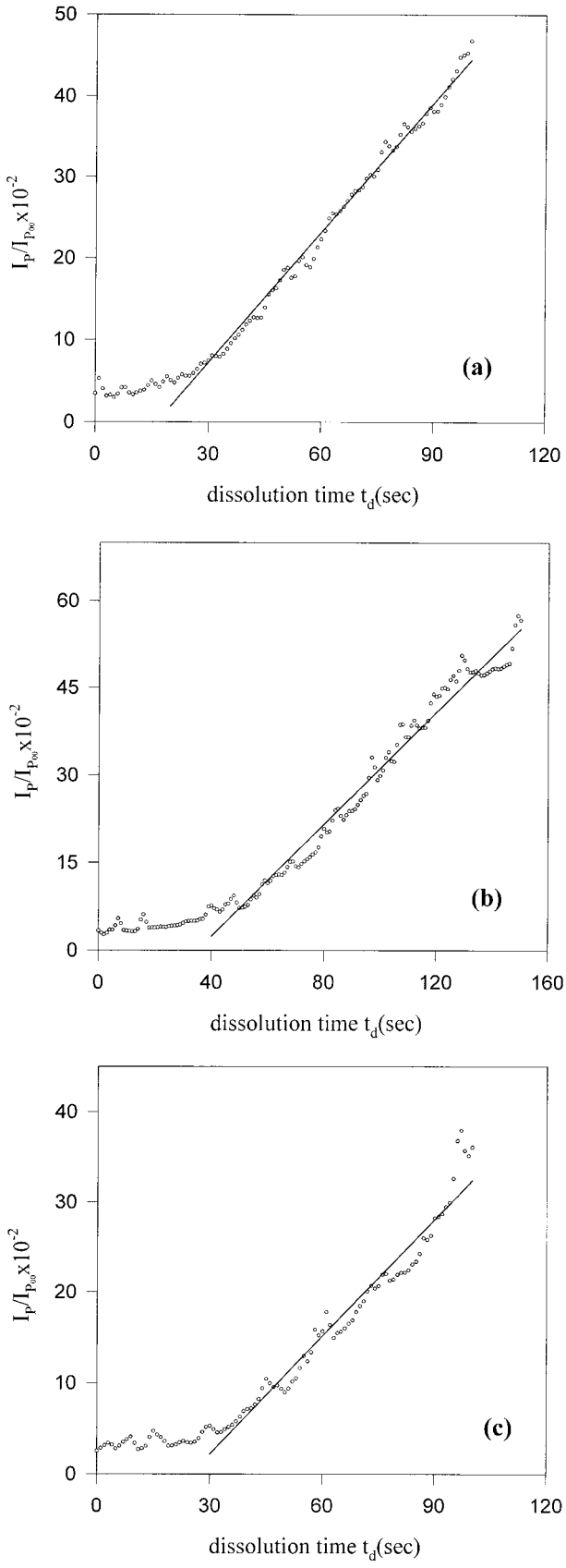

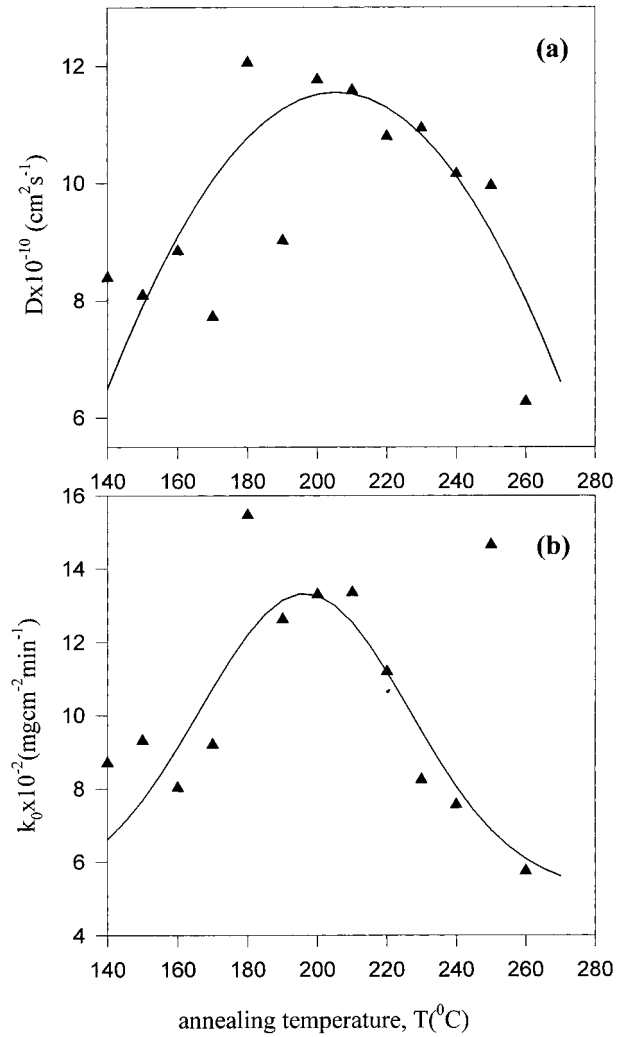

Figure 6 The plot of dissolution coefficients D_d (a) and relaxation parameters k_0 (b) against annealing temperatures.

one can observe behavior similar to that observed in D_d values; in other words, k_0 values are higher at intermediate temperatures and drop in the high-temperature region. A similar explanation is given as that for D_d values, in which small chains relax faster than large chains.

In Figure 5 all curves present a certain amount of delay in time axis, that is, formation of the swollen gel layer needs some time before the ad-

Figure 5 Comparison of early times region of the data in Figure 4(a)–(c) with the computations obtained by eq. (8). Relaxation constants k_0 are obtained from the slopes of the plots for the films annealed at (a) 150°C, (b) 190°C, and (c) 230°C.

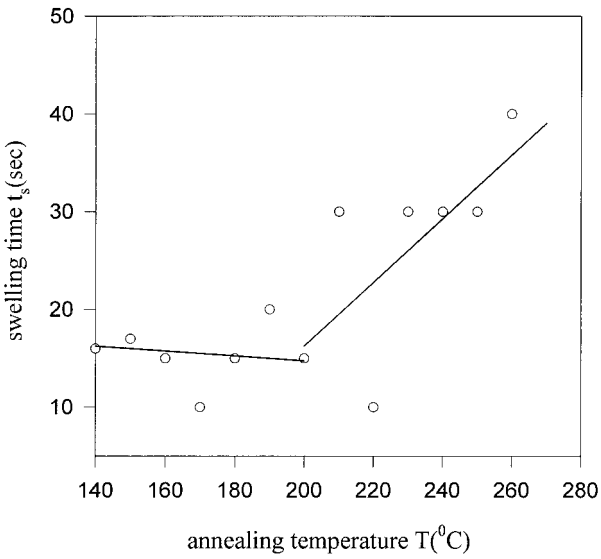

Figure 7 The plot of the swelling time t_s against annealing temperatures.

vancing boundary forms. The delay time in t_d is called swelling time (t_s), which is plotted versus annealing temperature T in Figure 7. It is observed that t_s remained almost constant up to 200°C then increased with increasing annealing temperature. This behavior of swelling film can be explained with the compactness of the annealed films, that is, films annealed at high temperatures ($T > 200$°C) need longer times to start swelling. Here by compactness we mean that films contain large, branched polymer chains.

In conclusion this study presents a work on latex film dissolution that can be used to extract some information during γ-ray treatment and annealing. At this stage of our experiments we have some difficulty of explaining the low annealing temperature behavior of dissolution.

REFERENCES

1. Eckersley, S. T.; Rudin, A. J Coatings Technol 1990, 62, 89.
2. Joanicot, M.; Wong, K.; Maquet, J.; Chevalier, Y.; Pichot, C.; Graillat, C.; Linder, P.; Rios, L.; Cabane, B. Prog Colloid Polym Sci 1990, 81, 175.
3. Sperry, P. R.; Snyder, B. S.; O'Down, M. L.; Lesko, P. M. Langmuir 1994, 10, 2619.
4. Mackenzie, J. K.; Shutlewort, R. Proc Phys Soc 1946, 62, 838.
5. Keddie, J. L.; Meredith, P.; Jones, R. A. L.; Ronald, A. M. in Proceedings of the American Chemical Society, Chicago, 1995.
6. Vanderhoff, J. W. Br Polym J 1970, 2, 161.
7. Kanig, G.; Neff, H. Colloid Polym Sci 1975, 256, 1052.
8. Wang, Y.; Kats, A.; Juhue, D.; Winnik, M. A.; Shivers, R. R.; Dinsdale, C. J. Langmuir 1992, 8, 1435.
9. Roulstone, B. J.; Wilkinson, M. C.; Hearn, J.; Wilson, A. J. Polym Int 1991, 24, 87.
10. Kim, K. D.; Sperling, L. H.; Klein, A. Macromolecules 1993, 26, 4624.
11. Pekcan, Ö.; Winnik, M. A.; Croucher, M. D. Macromolecules 1990, 23, 2673.
12. Wang, Y.; Zhao, C. L.; Winnik, M. A. J Chem Phys 1991, 95, 2143.
13. Wang, Y.; Winnik, M. A. Macromolecules 1993, 26, 3247.
14. Pekcan, Ö.; Canpolat, M.; Göçmen, A. Eur Polym J 1993, 29, 115.
15. Pekcan, Ö.; Canpolat, M.; Göçmen, A. Polymer 1993, 34, 3319.
16. Canpolat, M.; Pekcan, Ö. Polymer 1995, 36, 2025.
17. Pekcan, Ö. Trends Polym Sci 1994, 2, 236.
18. Pekcan, Ö.; Canpolat, M. Polym Adv Technol 1994, 5, 479.
19. Pekcan, Ö.; Kemeroğlu, F. J Appl Polym Sci 1999, 72, 981.
20. Pekcan, Ö.; Arda, E. J Appl Polym Sci 1998, 70, 339.
21. Pekcan, Ö.; Arda, E.; Kesenci, K.; Pişkin, E. J Appl Polym Sci 1998, 68, 1257.
22. Schnabel, W. in Degradation by High Energy Radiation; Jellinck, H. H. G., Ed.; Elsevier: Amsterdam, 1978.
23. Enscore, D. J.; Hopfenberg, H. B.; Stannett, V. T. Polymer 1977, 18, 793.
24. Thomas, N. L.; Windle, A. H. Polymer 1982, 23, 529.
25. Pekcan, Ö.; Uğur, Ş. J Appl Polym Sci 1998, 70, 1493.
26. Pekcan, Ö.; Uğur, Ş. Polymer 1997, 38, 5579.
27. Uğur, Ş.; Pekcan, Ö. Polymer, to appear.
28. Quano, A. C. Polym Eng Sci 1984, 18, 306.
29. Rodriguez, F.; Krasicky, P. D.; Groele, R. J. Solid State Technol 1985, May, 125.
30. Limm, W.; Dimnik, G. D.; Stanton, D.; Winnik, M. A.; Smith, B. A. J Appl Polym Sci 1988, 35, 2099.
31. Colombo, P.; Gazzaniga, A.; Caramella, C.; Conte, U.; Manna, A. L. Acta Pharm Technol 1987, 33, 15.
32. Krasicky, P. D.; Groele, R. J.; Rodriquez, F. J Appl Polym Sci 1988, 35, 641.
33. Guilet, J. E. in Photophysical and Photochemical Tools in Polymer Science; Winnik, M. A., Ed.; Reidel: Dordrecht, 1986.
34. Nivaggioli, T.; Wank, F.; Winnik, M. A. J Phys Chem 1992, 96, 7462.
35. Pascal, D.; Duhamel, J.; Wank, J.; Winnik, M. A.; Napper, Dh.; Gilbert, R. Polymer 1993, 34, 1134.
36. Lu, L.; Weiss, R. G. Macromolecules 1994, 27, 219.

37. Krongauz, V. V.; Mooney, W. F., III; Palmer, J. W.; Patricia, J. J. J Appl Polym Sci 1995, 56, 1077.
38. Krongauz, V. V.; Yohannan, R. M. Polymer 1990, 31, 1130.
39. He, Z.; Hammond, G. S.; Weiss, R. G. Macromolecules 1992, 25, 501.
40. Pekcan, Ö.; Canpolat, M.; Kaya, D. J Appl Polym Sci 1996, 60, 2105.
41. Pekcan, Ö.; Uğur, Ş.; Yilmaz, Y. Polymer 1997, 38, 2183.
42. Tu, Y. O.; Quano, A. C. IBM J Res Dev 1977, 21, 131.
43. Lee, P. I.; Peppas, N. A. J Controlled Release 1987, 6, 207.
44. Brochard, F.; de Gennes, P. G. Phys Chem Hydrodyn 1983, 4, 313.
45. Papanu, J. S.; Soane, D. S.; Bell, A. T. J Appl Polym Sci 1989, 38, 859.
46. Crank, J. The Mathematics of Diffusion; Clarendon Press: Oxford, 1975.
47. Winnik, M. A.; Hua, M. H.; Honhham, B.; Williamson, B.; Croucher, M. D. Macromolecules 1984, 17, 262.